Rev. Roum. Sci. Techn.– Électrotechn. et Énerg.
Vol. **64**, *4*, pp. 357–363, Bucarest, 2019

CLOSED LOOP DISCONTINUOUS PULSE WIDTH MODULATION CONTROL USED IN INVERTER GRID-CONNECTED PHOTOVOLTAIC SYSTEM FOR REDUCED SWITCHING LOSSES

SID-AHMED TOUIL[1], NASSERDINE BOUDJERDA[2], AHSENE BOUBAKIR[3], KHALIL EL KHAMLICHI DRISSI[4]

Keywords: Discontinuous pulse width modulation, Photovoltaic system, Sliding mode control, Switching losses, Dc-ac inverter.

This paper proposes a novel control of a direct grid-connected photovoltaic (PV) system using solely a three-phase inverter. Considering the large amount of energy transmitted to the network, we use the so-called discontinuous pulse width modulation (DPWM) technique for driving the inverter in closed loop, which reduces the number of commutations by about 33 %, resulting in an important decrease of the switching losses. The operation of the PV source at the maximum power point (MPP) and the control of the reactive energy injected into the network are performed using a designed robust sliding mode controller (SMC). The performances of the proposed system are evaluated through some simulation results, which highlight the effectiveness of the proposed SMC to achieve good control of the grid connected PV system. Additionally, the generalized discontinuous pulse width modulation strategy implemented in closed loop opens a new approach to the reduction of the switching losses in the PV inverter and may apply in other converters topologies for renewable energy systems.

1. INTRODUCTION

Nowadays, the use of renewable energy is growing rapidly. By powering millions of homes and businesses, they are reducing the air pollution, the global warming and the dependence on fossil fuels. Solar energy is an important part of renewable energies; it may be used directly for heating, lighting as well as for cooling. Moreover, grid-connected PV systems are the most popular solar electric sources. They deliver electric energy directly from the solar panel to the network without storage in batteries.

In practice, the current-voltage output characteristic (*I-V*) of a PV source is nonlinear and depends essentially on two parameters: the irradiance *G* and the temperature *T*. Also, this characteristic has a maximum power point (MPP), which should be achieved for optimal operation of the source [1]. Furthermore, the grid connection requires specific touches such as the control of the inverter output voltage and the control of reactive power by action on the phase shift between the voltage and the current at the grid input [2, 3], in addition to the reduction of the network harmonic pollution at low frequencies, which is limited by electromagnetic compatibility (EMC) standards for grid-connected decentralized sources [4, 5, 6]. Also, the switching losses in the power electronic converter need to be minimized seen the important amount of the energy transmitted to the network [7]. In order to satisfy these concerns, the grid-connected PV systems are currently the subject of many research works [3, 5, 8, 9].

Commonly, grid connected PV systems use two cascaded power electronic converters: a dc-dc converter for the control of the MPP of the PV source and a dc-ac converter allowing the control of the output voltage and the power factor as well as the reduction of the harmonic pollution of the output current [3, 9]. We notice that the use of powerful control techniques, allows removing the dc-dc converter; this provides more simplicity of the system, improves the overall efficiency and reduces the cost of the network connection [2, 9].

Operation of PV sources at the MPP is achieved by means of control algorithms called maximum power point trackers (MPPT) [10, 11]. The purpose is to reach accurate MPP as fast as possible; two simple algorithms with fixed step are widely used: the so called perturb and observe (P and O) [12] and the incremental conductance (IC) [13, 14]. However the fixed step size leads to a low dynamic response and generates oscillations at the steady state, which increases the power losses [10]; the use of variable step size enhances the dynamic performances and eliminates the oscillations; this enhances the accuracy of the MPPT and decreases the power losses [15].

Several closed loop schemes and techniques for the control of PV systems have been proposed in the literature [2, 3, 16, 17]. In [16] a basic proportional-integral (PI) controller is used to investigate the performance of a grid connected PV system by means of two cascaded dc-dc and dc-ac converters. In [2], the input-output feedback linearization technique is investigated to control both the power factor at the input of the grid and the MPPT of the PV source, using simply a dc-ac converter. The sliding mode control (SMC) is widely applied in nonlinear systems according to its robustness, simplified structure and easy implementation. A small scale PV system connected to a micro-grid using two cascaded dc-dc and dc-ac converters, is designed in [3] with both fuzzy logic control to regulate dc link voltage and sliding mode control to track permanently the MPP, an experimental validation is also achieved in [17].

In our work, we propose a grid connected PV system using only a three phase inverter with minimal switching losses. Considering the nonlinear behavior of the system, the SMC technique is used due to its remarkable properties [18, 19]. The proposed SMC algorithm achieves the control of both the power factor at the inverter output and the MPPT of the PV source; there is no need to use two separate algorithms for controlling these two variables. Also, the MPPT control is carried out directly via the dc-ac

[1] Department of Electrical Engineering, University Mohammed Seddik Ben Yahia Jijel, Algeria, sidahmed.touil1@gmail.com
[2] LER laboratory, University Mohammed Seddik Ben Yahia Jijel, Algeria
[3] LAJ laboratory, University Mohammed Seddik Ben Yahia Jijel, Algeria
[4] Pascal Institute, Blaise Pascal University, Clermont Ferrand, France

converter, therefore the dc-dc converter is removed, this provides a simple conversion system with a smaller bulk and lower cost, in addition it improves efficiency and reliability [2, 20]. The variable step IC MPPT algorithm is implemented due to its good performance in maintaining the maximum power point in various conditions. Knowing the significant amount of power injected into the network, we propose to drive the inverter using discontinuous pulse width modulation (DPWM), which reduces the number of commutations by about 33 %, resulting in an important decrease of the switching losses. In addition, the output voltage is increased by 15 %, compared to the well-known sinus-triangle PWM [21]. For this purpose a general algorithm of DPWM techniques that we call GDPWM is built in closed loop and the well-known particular schemes (DPWM0, DPWM1, DPWM2 and DPWM3) are deduced as particular cases [22, 23].

The main objectives and the novel contributions of this paper are summarized as follows:

- The design of a single SMC controller using directly the nonlinear model of the PV system and a single power electronic converter (inverter) for the grid connection, with the completion of three tasks: dc-ac voltage conversion, extraction of the maximum power from the PV source and regulation of the power factor in order to control the amount of the reactive power injected in the power network.
- The closed loop GDPWM technique to reduce the switching losses while maintaining the current ripple in the electromagnetic compatibility (EMC) the standards for grid-connected decentralized sources [4]; this opens a new field of innovation and investigation in renewable energy systems seen the large amount of energy involved.

The framework of the paper is organized as follows. Section 2 discusses the different parts of the proposed direct grid-connected PV source using a three-phase inverter with discontinuous PWM and a designed SMC. In Section 3, some simulation results of the proposed system are shown; its performances are highlighted and analyzed. Finally, the conclusions are reported in Section 4.

2. DIRECT GRID CONNECTED PHOTOVOLTAIC SOURCE USING THREE-PHASE INVERTER

The proposed three-phase grid-connected PV system is schematized in Fig. 1.

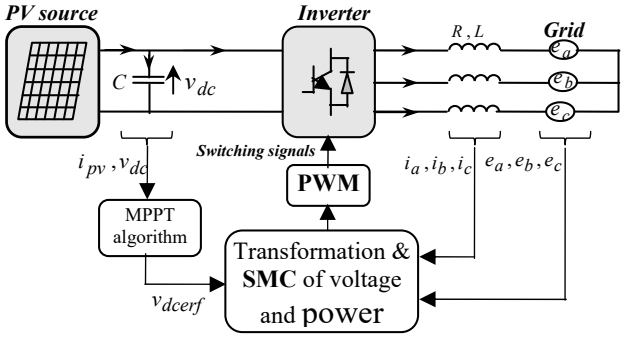

Fig. 1 – Direct grid connected PV source using three-phase inverter.

It consists of a solar array, a capacitive dc link and a three-phase inverter with inductive filter (*R, L*). The PV modules are connected in a series–parallel configuration to match the required dc voltage (v_{dc}) and power rating. Only a three-phase inverter is required, which provides a simple conversion system.

2.1. PHOTOVOLTAIC SOURCE

PV cells are the smallest units of PV sources. To obtain the characteristics and the behavior of a PV cell, we use the simplified real model illustrated in Fig. 2 [2].

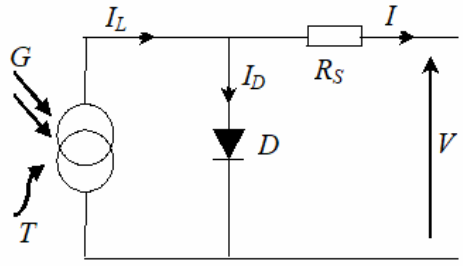

Fig. 2 – Circuit diagram of the PV cell model.

The modeling of the solar cell is defined by the following voltage–current relationship:

$$I = I_L - I_0\left(e^{q(V+I\,R_S)/nkT} - 1\right), \tag{1}$$

where I_L is the photocurrent generated by the current source (A), I_0 is the saturation current of the diode (A), q is the electron charge (1.60217 10^{-19} C), R_s is a series resistance (Ω), n is the diode quality factor, k is the Boltzmann's constant (1.38065 10^{-23} J/K) and T is the cell temperature (K).

The model includes temperature and irradiance dependence as follows:

$$I_L = I_{L(T_1)}\left(1 + K_0\left(T - T_1\right)\right), \tag{2}$$

$$I_{L(T_1)} = G * I_{SC(T_1,nom)} / G_{(nom)}\,, \tag{3}$$

$$K_0 = \left(I_{SC(T_2)} - I_{SC(T_1)}\right) / \left(T_2 - T_1\right), \tag{4}$$

$$I_0 = I_{0(T_1)} * \left(T/T_1\right)^{3/n} * e^{-q\,V_g/n\,k*(1/T - 1/T_1)}, \tag{5}$$

$$I_0(T_1) = I_{SC(T_1)} \Big/ \left(e^{q\,V_{OC(T_1)}/nkT_1} - 1\right), \tag{6}$$

where G and $G_{(nom)}$ are the irradiance and the nominal irradiance in (W/m^2), T_2 and T_1 are the temperature references; they are calculated from the datasheet parameters, in our case: T_2 = 75 ^{0}C and T_1 = 25 ^{0}C, $I_{SC(T2,nom)}$, $I_{SC(T1)}$ and $I_{SC(T2)}$ are the short circuit currents at the corresponding temperatures under an irradiance G = 1 kW/m^2, $I_{L(T1)}$, $I_{0(T1)}$ and $V_{OC(T1)}$ are the photocurrent, the saturation current and the open circuit voltage at a temperature T_1 and V_g is the band gap voltage.

More details on the modeling of a PV cell can be found in [2]. In our work, we use the BP3160 modules, which parameters are detailed in the datasheet (Table 1). Using the equations (1) to (6), the current-voltage (*I-V*) and the power-voltage (*P-V*) characteristics of the studied array, related to both temperature *T* and irradiation *G* are shown in Fig. 3. This array is composed of 5 parallel groups of modules; each group contains 30 modules in series.

Table 1
Parameters of PV module BP3160 (G = 1 kW/m^2 and T = 25 ^{0}C).

Parameter	Value
Typical peak power	160 W
Voltage at peak power	35.1 V
Current at peak power	4.55 A
Short circuit current	4.8 A
Open circuit voltage	44.2 V
Temperature coefficient of I_{sc}	(0.065 ± 0.015)%/^{0}C
Nominal operating cell temperature (T_{ref})	47 ± 2^{0}C

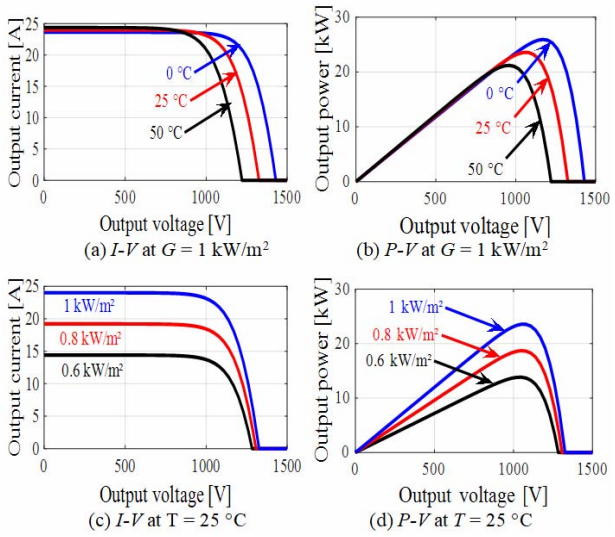

(a) I-V at G = 1 kW/m^2 (b) P-V at G = 1 kW/m^2
(c) I-V at T = 25 °C (d) P-V at T = 25 °C
Fig. 3 – PV array characteristics.

2.2. INCREMENTAL CONDUCTANCE ALGORITHM

It is paramount to operate the PV sources at the maximum power point (MPP). Several MPPT algorithms are proposed in the literature [15, 24]. In our work, a very effective MPPT method is used: the so-called incremental conductance MPPT with variable step size [24]. The IC MPPT algorithm is based on the knowledge and the comparison between the instantaneous conductance $G = I/V$ of the PV source and the incremental conductance $\Delta G = \Delta I/\Delta V$. The MPP is reached once the instantaneous conductance equals the incremental one with a minus sign.

Note: The traditional MPPT algorithms fail to track the peak control variable under fast varying conditions by generation of oscillations around MPP [24]. To alleviate this drawback and to ensure a rapid and accurate tracking, the variable step IC MPPT is adopted in this work.

The used variable step size method is the following [23]:

$$v_{dcref}(k) = v_{dcref}(k-1) \pm N * \left| \frac{\Delta P_{PV}}{\Delta v_{dc} - \Delta i_{PV}} \right|,$$

where $v_{dcref}(k)$ and $v_{dcref}(k\text{-}1)$ are the voltage references at the step (k) and the previous step (k – 1), respectively. N is the scaling factor manually adjusted at the sampling period to regulate the step size. ΔP_{PV}, Δv_{dc} and Δi_{PV} are the power, voltage and current variations between the present and previous steps respectively, given by:

$$\Delta P_{PV} = P_{PV}(k) - P_{PV}(k-1),$$
$$\Delta v_{dc} = v_{dc}(k) - v_{dc}(k-1),$$
$$\Delta i_{PV} = i_{PV}(k) - i_{PV}(k-1).$$

2.3. THREE-PHASE INVERTER AND GDPWM ALGORITHM DEVELOPMENT

The three-phase two-level inverter is presented in Fig. 4(a). Each of the three legs requires two control signals:

$$q_{i2} = \overline{q_{i1}}, \; i = 1, 2, 3. \qquad (7)$$

Commonly, the triangle-sinus modulation (TSM) and the space vector modulation (SVM) are used to generate the switching signals. In practice, SVM allows extending the linearity up to $\left(2/\sqrt{3} \approx 1.15\right)$ and can be implemented either by numerical software or by analog devices; this last method is called hybrid space vector modulation (HSVM) and derives from the TSM by adding an adequate zero sequence to the sine references for each phase [23].

For high power levels, such as grid connected renewable energy sources, the switching losses are very significant. We propose to reduce these losses by using the so called DPWM technique, which consists on a clamping of the reference signals at the maximum (or the minimum) value during a phase angle of $2\pi/3$; this leads to a no-commutation during this angle, thereby canceling the switching losses [6, 22]. The principle of DPWM techniques consists on the injection of a zero sequence reference v_{zs}^{**} in the sinusoidal references v_{abc}^{*} in the same way of the HSVM [23]. The only difference is in the derivation of the zero sequence, (Fig. 4(b) and (c)). The main features of this technique are [23]:

- The extending of the linearity up to $2/\sqrt{3}$ as in SVM.
- The reduction of the number of commutations per 33 % symmetrically in the two half-cycles: all switches are inactive during a phase angle of b $\pi/3$ [6]; this is the main purpose of this technique because it allows an important reduction of the switching losses while maintaining a symmetrical operation of all switches.

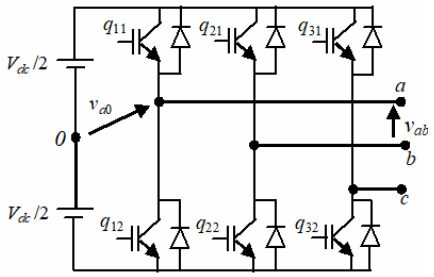

(a) three-phase inverter.

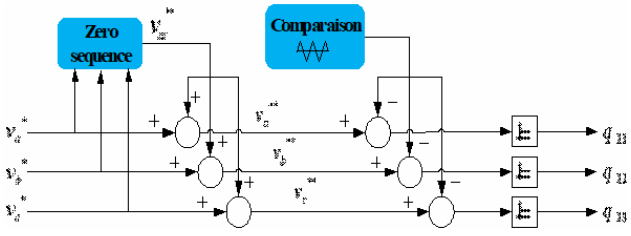

(b) Principle of GDPWM technique.

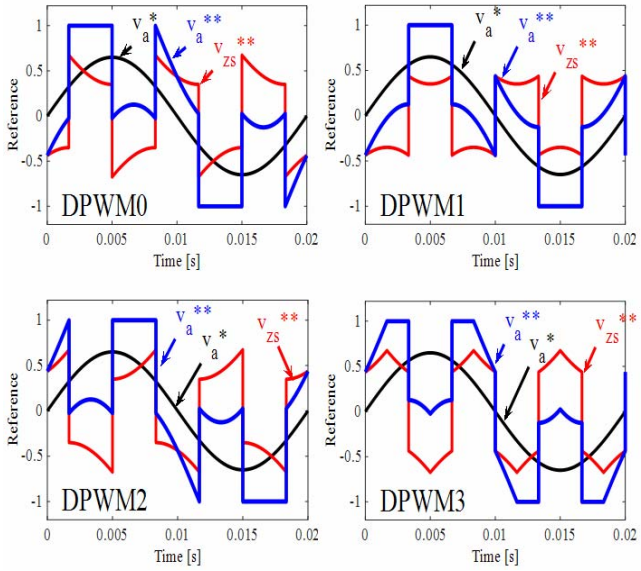

(c) References of particular DPWM schemes.

Fig. 4 –Three-phase inverter and GDPWM technique.

In this work, we have developed a general algorithm for DPWM techniques that we call GDPWM; allowing online generation of various closed loop DPWM reference signals (Fig. 4(b)). The well-known particular DPWM schemes (DPWM0, DPWM1, DPWM2 and DPWM3) are obtained directly as particular cases. The initial sinusoidal reference v_a^*, the zero sequence signal v_{zs}^{**} and the final DPWM reference v_a^{**} (modulating waveform for phase *a*) are shown in Fig. 4(c) for these particular schemes.

2.4. DESIGN OF SLIDING MODE CONTROLLER FOR THE PV SYSTEM

The overall aim is to design a controller that ensures the PV source to operate at the maximum power point extracted by the MPPT and to maintain the power factor at a desired value, which allows the control of the reactive power injected in the network. We use the theory of SMC to develop a robust control law. The SMC is an important method of nonlinear control, due to its inherent advantages, *e.g.* robustness, disturbance resistance, convergence, insensitivity to the parameters variations and non-linearity. SMC alters the system dynamics by forcing it to enter and then slide along a surface, on which the system has the desired properties such as stability and disturbance resistance. In order to design the SMC controller, let's consider the electrical equations of the inverter output voltage (Fig. 1):

$$\begin{cases} v_a = R\,i_a + L\dfrac{\mathrm{d}i_a}{\mathrm{d}t} + e_a \\ v_b = R\,i_b + L\dfrac{\mathrm{d}i_b}{\mathrm{d}t} + e_b \\ v_c = R\,i_c + L\dfrac{\mathrm{d}i_c}{\mathrm{d}t} + e_c \end{cases}. \tag{8}$$

By applying the Park transformation to eq. (8) and Kirchhoff's laws at the inverter dc inside, we obtain [10]:

$$\begin{cases} L\dfrac{\mathrm{d}i_d}{\mathrm{d}t} + R\,i_d - \omega L\,i_q + e_d = v_d \\ L\dfrac{\mathrm{d}i_q}{\mathrm{d}t} + R\,i_q + \omega L\,i_d + e_q = v_q \\ C\dfrac{\mathrm{d}v_{dc}}{\mathrm{d}t} = i_{pv} - \dfrac{e_d.i_d + e_q.i_q}{v_{dc}} \end{cases}. \tag{9}$$

After some mathematical transformations, the state model of the inverter connected to the dc link bus v_{dc} and the grid, can be written using the following compact form:

$$\dot{x} = f(x) + g(x)\,u\,, \tag{10}$$

where $x = (x_1, x_2, x_3)^{\mathrm{T}} = (i_d, i_q, v_{dc})^{\mathrm{T}}$ is the state vector and $u = (u_1, u_2)^{\mathrm{T}} = (v_d, v_q)^{\mathrm{T}}$ is the input vector. The vector fields are defined as follows:

$$f(x) = \begin{pmatrix} f_1(x) \\ f_2(x) \\ f_3(x) \end{pmatrix} = \begin{pmatrix} -\dfrac{R}{L}\cdot x_1 + \omega\cdot x_2 - \dfrac{e_d}{L} \\ -\dfrac{R}{L}\cdot x_2 + \omega\cdot x_1 - \dfrac{e_q}{L} \\ \dfrac{i_{pv}}{C} - \dfrac{e_d\cdot x_1 + e_q\cdot x_2}{C\cdot x_3} \end{pmatrix},\quad g(x) = \begin{pmatrix} \dfrac{1}{L} & 0 \\ 0 & \dfrac{1}{L} \\ 0 & 0 \end{pmatrix}.$$

The two states x_2 and x_3 are considered as the outputs of the model such that: $y = (y_1, y_2)^{\mathrm{T}} = (x_2, x_3)^{\mathrm{T}} = (i_q, v_{dc})^{\mathrm{T}}$.

Since the relative degrees of y_1 and y_2 are r_1=1 and r_2=2 respectively, the dynamic system given by eq. (10) can be rewritten in the following input-output form:

$$\begin{pmatrix} \dot{y}_1 \\ \ddot{y}_2 \end{pmatrix} = E(x) + B(x)\,u\,, \tag{11}$$

$B(x)$ is a nonsingular decoupling matrix, where:

$$E(x) = \begin{pmatrix} f_2 \\ \dfrac{\dot{i}_{pv}}{C} - \dfrac{1}{C\cdot x_3}\left(e_d\cdot f_1 + e_q\cdot f_2\right) + \dfrac{\left(e_d\cdot x_1 + e_q\cdot x_2\right)}{C\cdot {x_3}^2}\cdot f_3 \end{pmatrix},$$

$$B(x) = \begin{pmatrix} 0 & \dfrac{1}{L} \\ -\dfrac{e_d}{LCx_3} & \dfrac{e_q}{LCx_3} \end{pmatrix}.$$

Let us define the tracking errors as $e_1 = i_{qref} - i_q$ and $e_2 = v_{dcref} - v_{dc}$ and the sliding surfaces as:

$$S = \begin{pmatrix} S_1 \\ S_2 \end{pmatrix} = \begin{pmatrix} e_1 \\ \dot{e}_2 + \lambda\, e_2 \end{pmatrix}, \tag{12}$$

where $\dot{e}_2$ is the time derivative of the error e_2.

The time derivatives of the filtered errors of eq. (12) can be rewritten as:

$$\dot{S} = \begin{pmatrix} \dot{S}_1 \\ \dot{S}_2 \end{pmatrix} = \begin{pmatrix} \dot{i}_{qref} \\ \ddot{V}_{dcref} + \lambda\,\dot{e}_2 \end{pmatrix} - E(x) - B(x).u\,. \tag{13}$$

Based on the sliding mode control theory, we propose the following robust control law:

$$u=\begin{pmatrix}u_1\\u_2\end{pmatrix}=B^{-1}\left[\begin{pmatrix}\dot{i}_{qref}\\ \ddot{V}_{dcref}+\lambda\dot{e}_2\end{pmatrix}-E+K_0\cdot S+K\cdot\tanh\left(\frac{S}{\varepsilon_0}\right)\right] \quad (14)$$

where:

- $K_0=\begin{pmatrix}K_{01}&0\\0&K_{02}\end{pmatrix}$ and $K=\begin{pmatrix}K_1&0\\0&K_2\end{pmatrix}$.
- $K_{0i}>0$ and $K_i>0$ for i =1, 2, and ε_0 is a small positive constant.
- $\tanh(\cdot)$ is the hyperbolic tangent function defined for the vector $S=(S_1,S_2)^{\mathrm{T}}$ as:

$$\tanh\left(\frac{S}{\varepsilon_0}\right)=\left(\tanh\left(\frac{S_1}{\varepsilon_0}\right),\tanh\left(\frac{S_2}{\varepsilon_0}\right)\right)^{\mathrm{T}}.$$

The selected control input u in eq. (14) is replaced in eq. (13), this last simplifies to:

$$\dot{S}=-K_0\cdot S-K\cdot\tanh\left(\frac{S}{\varepsilon_0}\right). \quad (15)$$

According to eq. (15) we conclude that $S_1\to 0$ as $t\to\infty$ and therefore, both $e_1=i_{qref}-i_q$ and $e_2=v_{dcref}-v_{dc}$ converge to zero.

Note: $\tanh(\cdot)$ is a smooth approximation of the discontinuous term "$\mathrm{sign}(\cdot)$", which may cause oscillations of the trajectories system around the sliding surface. This smoother variator is usually used in robust control to eradicate the chattering phenomenon that occurs in the sliding mode system [25].

3. SIMULATION RESULTS AND ANALYSIS

In this section, some simulation results are presented and discussed. Firstly, we present the performances of the control of both the input voltage and the power factor using the nonlinear SMC technique. Secondly, the effect of the MPPT algorithm is observed on both the control performance and the low order harmonic distortion of the grid current i_a (phase a). Thirdly, the GDPWM technique presented in Section 2.3 is exploited in closed loop; some results concerning the particular DPWM schemes are compared to the classical TSM technique taken as a benchmark. The comparison is based on the reduction of the number of commutations as well as the spectrum of the grid current i_a so as to comply with EMC standards for grid connected renewable energy sources [4, 5].

3.1. PERFORMANCE OF THE SLIDING MODE CONTROL

We present the simulation results of the control of both the dc bus voltage v_{dc} to get the MPP and the power factor at the inverter output at a wanted value (the max value is the unity; it corresponds to i_q = 0). There is no significant effect of the discontinuous PWM techniques on the sliding mode control performance (negligible effect), the results of Fig. 5 correspond to the classical PWM technique. Three perturbations are considered: firstly with change of the irradiation from G = 1 kW/m² to 0.4 kW/m², between t = 0.4 s and t = 0.6 s, then the temperature change from T = 25°C to 50 °C, between 0.8 s and 1 s, finaly with i_{qref} change from i_{qref} = 0 A to 50 A, between 1.2 and 1.4 s.

The dc voltage (v_{dc}) perfectly tracks the reference voltage in order to operate at the MPP (Fig. 5(a)), while i_q is not affected by the changes of both irradiation G and temperature T; i_q and i_{qref} are superimposed regardless to the perturbations, (G and T changes), (Fig. 5(e)). We notice that the effect of the irradiation is more important than that of the temperature on the MPP (Figs. 5(b) and (c)). On the other side, the change of i_q reference has no effect on the voltage v_{dc} and the power P_{PV}, it only affects the amplitude and the phase of the grid current i_a (Fig. 5(f)); this is predictable because it corresponds only on the reactive power injected in the grid.

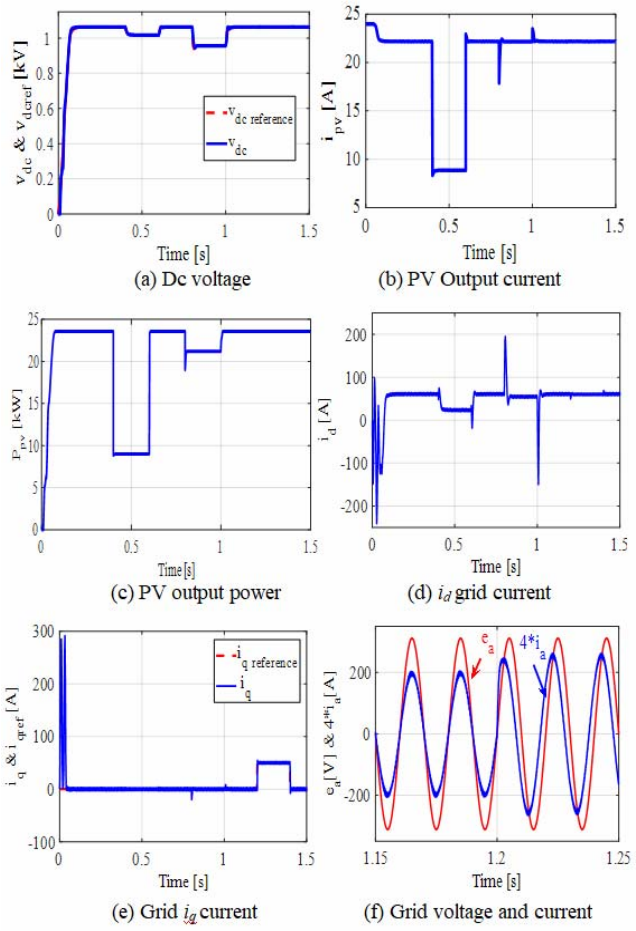

Fig. 5 – SMC performance using classical PWM.

3.2. REDUCTION OF SWITCHING LOSSES USING DPWM TECHNIQUES

Figure 6(a) shows the reference signals for the particular closed loop DPWM schemes (DPWM0, DPWM1, DPWM2 and DPWM3) and Fig. 6(b) shows the corresponding switching signals using a triangular carrier of 3 kHz. A perfect correlation is reached between the open loop references (Fig. 4(c)) and closed loop (Fig. 6(a)). We see also in Fig. 6(b) the no-switching sequences (corresponding to the minimum or maximum clamping of the references).

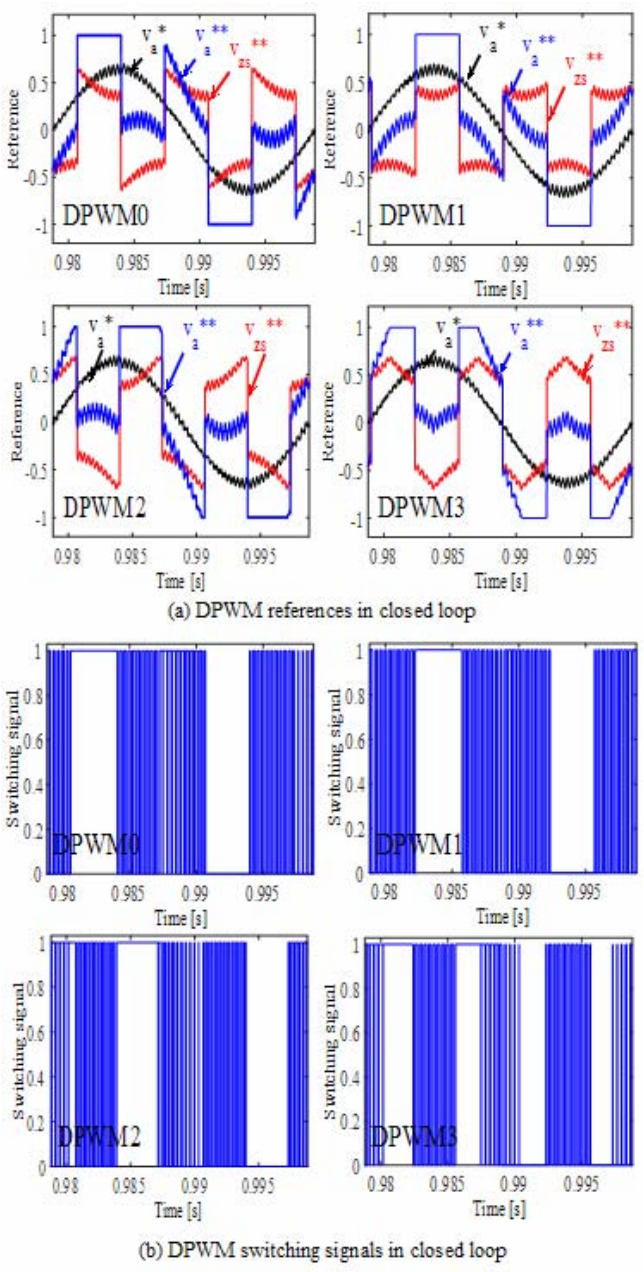

Fig. 6 – GDPWM closed loop switching signals.

For the classical PWM and for all DPWM techniques, the current waveforms and their spectra are given in Fig. 7. The spectra comply perfectly with the requirements of "IEEE Std Harmonic Limits" [4] in which, the THD is limited to 5 % and each individual harmonic is limited to 3 %. In addition, a comparison between the different schemes in closed loop is presented in Table 2; this comparison is based both on the number of commutations per fundamental period and on the THD of the grid current. All DPWM schemes allow a reduction of commutations by about 33 %, while all the THDs and individual harmonics comply with "IEEE Std Harmonic Limits" [4, 5].

Note: The GDPWM algorithm is directly inserted in the closed loop and the well known schemes (DPWM0, DPWM1, DPWM2 and DPWM3) are deduced as particular cases.

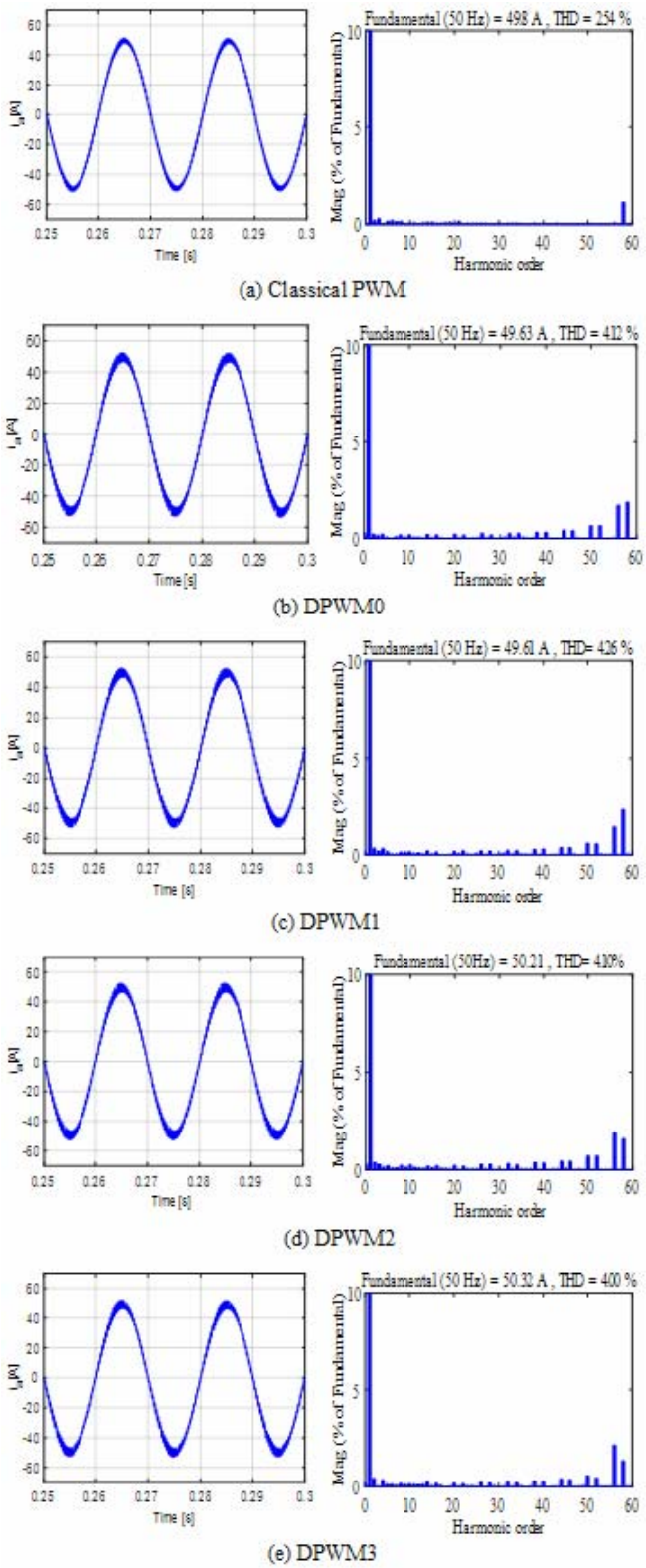

Fig. 7 – Grid currents waveforms and spectra.

Table 2

Comparison of particular DPWM schemes

PWM technique	TSM	DPWM0	DPWM1	DPWM2	DPWM3
THD (%)	2.54	4.12	4.26	4.10	4.00
Number of commutations / period	120	82	82	80	80

Finally, we note the following strengths of the proposed system:

- The SMC of both the dc bus voltage and the i_q current gives satisfactory performances regardless to the PWM techniques (triangle-sinus PWM or DPWM).
- The use of an inverter only (without dc-dc converter) simplifies considerably the PV system.
- The reduction of the switching losses in the inverter using closed-loop GDPWM techniques is paramount due to the power amount transmitted to the network.

4. **CONCLUSION**

Our objective is to propose an efficient closed-loop control technique for a PV source connected directly to the network, using just a three-phase inverter with minimal switching losses.

The designed SMC technique controls both the output voltage of the PV source and the grid current, in order to extract the maximum power using appropriate MPPT and to regulate the reactive power injected in the network. Further, a new application of DPWM techniques is proposed in closed loop to minimize the inverter switching losses, given the large amount of energy transmitted to the network.

Simulation results show very good performance of the SMC technique. Furthermore, the use of the closed loop DPWM techniques allows reducing the number of commutations by 33 % that results in an important reduction of the switching losses, while maintaining a good quality of the electrical energy.

Received on March 13, 2018

REFERENCES

1. M. de Brito, L. Galotto, L. Sampaio, G. e Melo, C. Canesin, *Evaluation of the Main MPPT Techniques for Photovoltaic Applications*, IEEE Transactions On Industrial Electronics, **60**, pp. 1156–1167 (2013).
2. D. Lalili, A. Mellit, N. Lourci, B. Medjahed, E. Berkouk, *Input output feedback linearization control and variable step size MPPT algorithm of a grid-connected photovoltaic inverter*, Renewable Energy, **36**, pp. 3282–3291 (2011).
3. A. Menadi, S. Abdeddaim, A. Ghamri, A. Betka, *Implementation of fuzzy-sliding mode based control of a grid connected photovoltaic system*, ISA Transactions, **58**, pp. 586–594 (2015).
4. IEEE application guide for IEEE Std 1547™, *IEEE standard for interconnecting distributed resources with electric power systems*, 1st ed. New York, NY: Institute of Electrical and Electronics Engineers, pp. 1–217 (2009).
5. V. Lal, S. Singh, *Control and Performance Analysis of a Single-Stage Utility-Scale Grid-Connected PV System*, IEEE Systems Journal, pp. 1–11 (2015).
6. A. Boudouda, N. Boudjerda, A. Aibeche, A. Bouzida, *Dual randomized pulse width modulation technique for buck converter fed by photovoltaic source*, Rev. Roum. Sci. Techn. – Électrotechn. et Énerg., **63**, *3*, pp. 289–294 (2018).
7. Y. Wu, M. Shafi, A. Knight, R. McMahon, *Comparison of the Effects of Continuous and Discontinuous PWM Schemes on Power Losses of Voltage-Sourced Inverters for Induction Motor Drives*, IEEE Transactions On Power Electronics, **26**, pp. 182–191 (2011).
8. S. Kim, J. Park, K. Lee, T. Kim, Novel pulse-width modulation strategy to minimize the switching losses of Z-source inverters, Electr. Power Components Syst., **42**, pp. 1213–1225 (2014).
9. A. Radwan, Y. Mohamed, *Power Synchronization Control for Grid-Connected Current-Source Inverter-Based Photovoltaic Systems*, IEEE Transactions On Energy Conversion, **31**, pp. 1023–1036 (2016).
10. D. Ouoba, A. Fakkar, Y. El Kouari, F. Dkhichi, B. Oukarfi, *An improved maximum power point tracking method for a photovoltaic system*, Optical Materials, **56**, pp. 100–106 (2016).
11. P. Chen, P. Chen, Y. Liu, J. Chen, Y. Luo, *A comparative study on maximum power point tracking techniques for photovoltaic generation systems operating under fast changing environments*, Solar Energy, **119**, pp. 261–276 (2015).
12 A. F. Murtaza, M. Chiaberge, F. Spertino, U. Tabrez, D. Boero, M. De Giuseppe, *MPPT technique based on improved evaluation of photovoltaic parameters for uniformly irradiated photovoltaic array*, Electric Power System Research, **145**, pp. 248–263 (2017).
13. R. Faraji, M. Chavoshian, A. Rouholamini, H. Naji, R. Fadaeinedjad, *FPGA-based real time incremental conductance maximum power point tracking controller for photovoltaic systems*, IET Power Electronics, **7**, pp. 1294–1304 (2014).
14. P. Sivakumar, A. Abdul Kader, Y. Kaliavaradhan, M. Arutchelvi, *Analysis and enhancement of PV efficiency with incremental conductance MPPT technique under non-linear loading conditions*, Renewable Energy, **81**, pp. 543–550 (2015).
15. S. Saravanan, N. Ramesh Babu, *Maximum power point tracking algorithms for photovoltaic system – A review*, Renewable And Sustainable Energy Reviews. **57**, pp. 192–204 (2016).
16. P. Sarothi sikder, N. Pal, *Incremental conductance based maximum power point tracking controller using different buck-boost converter for solar photovoltaic system*, Rev. Roum. Sci. Techn. – Électrotechn. et Énerg., **62**, *3*, pp. 269–275 (2017).
17 S. Ouchen, S. Abdeddaim, A. Betka, A. Menadi, *Experimental validation of sliding mode-predictive direct power control of a grid connected photovoltaic system, feeding a nonlinear load*, Solar Energy, **137**, pp. 328–336 (2016).
18. A. M. Nader, A. Dib, *Direct power control for a photovoltaic conversion chain connected to a grid,* Rev. Roum. Sci. Techn. – Électrotechn. et Énerg, **61**, *4*, pp. 378–382 (2016).
19. A. Aberbour, k. Idjdarene, Z. Boudries, *Adaptable sliding mode control for wind energy application,* Roum. Sci. Techn. – Électrotechn. et Énerg, **61**, *3*, pp. 258–262 (2016).
20 Z. Zeng, H. Yang, R. Zhao, C. Cheng, *Topologies and control strategies of multi-functional grid-connected inverters for power quality enhancement: A comprehensive review*, Renewable And Sustainable Energy Reviews, **24**, pp. 223–270 (2013).
21 C. Yan, C. Sun, Y. Zhang, M. Chen, D. Xu, *A hybrid PWM modulation scheme for PV inverter*, In: IEEE 1st International Future Energy Electronics Conference, IFEEC, pp. 406–410 (2013).
22. T. Bramhananda Reddy, K. Ishwarya, D. Vyshnavi, K. Haneesha, *Generalized scalar PWM algorithm for three-level diode clamped inverter fed induction motor drives with reduced complexity*, In: IEEE Intern. Conf. on Advances in Power Conv. and Energy Tech. (APCET), Mylavaram, Andhra Pradesh, pp. 1–6 (2012).
23. V. Blasko, *Analysis of a hybrid PWM based on modified space-vector and triangle-comparison methods*, IEEE Transactions on Industry Applications, **33**, pp. 756–764 (1997).
24. A. Loukriz, M. Haddadi, S. Messalti, *Simulation and experimental design of a new advanced variable step size Incremental Conductance MPPT algorithm for PV systems*, ISA Transactions, **62**, pp. 30–38 (2016).
25. N. Hamidreza, B. Mai, H.Shinji, *Chattering attenuation sliding mode approach for nonlinear systems*, Asian J. Control, **19**, *4*, pp. 1519–1531 (2017).